

Experimental demonstration of an analytic method for image reconstruction in optical tomography with large data sets

Zheng-Min Wang, George Y. Panasyuk, Vadim A. Markel and John C. Schotland

*Departments of Bioengineering and Radiology
University of Pennsylvania, Philadelphia, PA 19104*

(Dated: September 27, 2018)

We report the first experimental test of an analytic image reconstruction algorithm for optical tomography with large data sets. Using a continuous-wave optical tomography system with 10^8 source-detector pairs, we demonstrate the reconstruction of an absorption image of a phantom consisting of a highly-scattering medium with absorbing inhomogeneities.

Optical tomography (OT) is a biomedical imaging modality that utilizes diffuse light as a probe of tissue structure and function[1]. Clinical applications include imaging of breast disease and functional neuroimaging. The physical problem that is considered is to reconstruct the optical properties of an inhomogenous medium from measurements taken on its surface. In a typical experiment, optical fibers are used for illumination and detection of the transmitted light [2, 3, 4]. The number of measurements (source-detector pairs) which can be obtained, in practice, varies between $10^2 - 10^4$. A recently proposed alternative to fiber-based experiments is to employ a narrow incident beam for illumination. The beam can be scanned over the surface of the medium while a lens-coupled CCD detects the transmitted light. Using such a “noncontact” method, it is possible to avoid many of the technical difficulties which arise due to fiber-sample interactions [5, 6, 7, 8]. In addition, extremely large data sets of approximately $10^8 - 10^{10}$ measurements can readily be obtained. Data sets of this size have the potential to vastly improve the quality of reconstructed images in OT.

The reconstruction of images from large data sets is an extremely challenging problem due to the high computational complexity of numerical approaches to the inverse problem in OT. To address this challenge, we have developed analytic methods to solve the inverse problem [9, 11, 12]. These methods lead to a dramatic reduction in computational complexity and have been applied in numerical simulations to data sets as large as 10^{10} measurements [11]. In this Letter, we report the first experimental test of an analytic image reconstruction method. By employing a noncontact OT system with 10^8 source-detector pairs, we reconstruct the optical absorption of a highly-scattering medium. The results demonstrate the feasibility of image reconstruction for OT with large data sets.

We begin by considering the propagation of diffuse light. The density of electromagnetic energy $u(\mathbf{r})$ in an absorbing medium obeys the diffusion equation

$$-D\nabla^2 u(\mathbf{r}) + \alpha(\mathbf{r})u(\mathbf{r}) = S(\mathbf{r}), \quad (1)$$

where $\alpha(\mathbf{r})$ is the absorption coefficient, $S(\mathbf{r})$ is the power density of a continuous wave source, and D is the diffu-

sion constant. The energy density also obeys the boundary condition $u + \ell \hat{\mathbf{n}} \cdot \nabla u = 0$ on the surface bounding the medium, where $\hat{\mathbf{n}}$ is the unit outward normal and ℓ is the extrapolation length [10]. The relative intensity measured by a point detector at \mathbf{r}_2 due to a point source at \mathbf{r}_1 is given, within the accuracy of the first Rytov approximation, by the integral equation

$$\phi(\mathbf{r}_1, \mathbf{r}_2) = \int d^3r G(\mathbf{r}_1, \mathbf{r}) G(\mathbf{r}, \mathbf{r}_2) \delta\alpha(\mathbf{r}), \quad (2)$$

where the source and detector are oriented in the inward and outward normal directions, respectively [12]. Here $\delta\alpha(\mathbf{r}) = \alpha(\mathbf{r}) - \alpha_0$ denotes the spatial fluctuations in $\alpha(\mathbf{r})$ relative to a reference medium with absorption α_0 , G is the Green’s function for Eq. (1) with $\alpha = \alpha_0$, and the data function ϕ is defined by $\phi(\mathbf{r}_1, \mathbf{r}_2) = -G(\mathbf{r}_1, \mathbf{r}_2) \ln(I(\mathbf{r}_1, \mathbf{r}_2)/I_0(\mathbf{r}_1, \mathbf{r}_2))$, where $I(\mathbf{r}_1, \mathbf{r}_2)$ denotes the intensity in the medium and $I_0(\mathbf{r}_1, \mathbf{r}_2)$ is the intensity in the reference medium. Note that the intensity is related to the Green’s function by the expression

$$I(\mathbf{r}_1, \mathbf{r}_2) = \frac{cS_0}{4\pi} \left(1 + \frac{\ell^*}{\ell}\right)^2 G(\mathbf{r}_1, \mathbf{r}_2), \quad (3)$$

where S_0 is the source power and the transport mean free path ℓ^* is related to the diffusion coefficient by $D = 1/3c\ell^*$.

We have constructed a noncontact OT system to test the analytic method of image reconstruction. A schematic of the instrument is shown in Fig. 1. The source is a continuous-wave stabilized diode laser (DL7140-201, Thorlabs) operating at a wavelength of 785 nm with an output power of 70 mW. The laser output is divided into two beams by a beam splitter. The reflected beam is incident on a power meter which monitors the stability of the laser intensity. The transmitted beam passes through a lens onto a pair of galvanometer-controlled mirrors (SCA 750, Lasesys). The mirrors are used to scan the beam, which has a focal spot size of 200 μm , in a raster fashion over the surface of the sample. After propagating through the sample, the transmitted light passes through a band-pass interference filter (10LF20-780, Newport) and is imaged onto a front illuminated thermoelectric-cooled 16-bit CCD array (DV435,

Andor Technology) using a 23 mm/ $f1.4$ lens. A mechanical shutter is placed in front of the CCD to reduce artifacts associated with frame transfer within the CCD chip. A pulse generator with digital delay is used to trigger and synchronize the CCD, the shutter and the position of the beam.

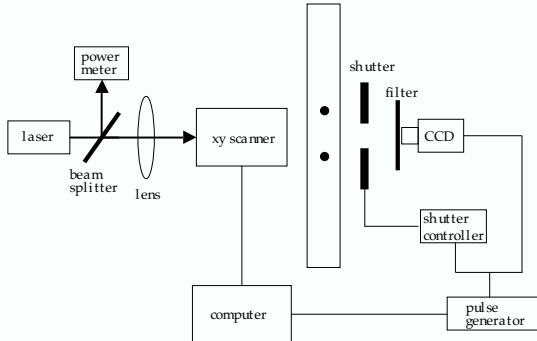


Fig. 1. Schematic of the noncontact optical tomography system.

The sample chamber is a rectangular box of depth 5 cm with square faces of area $50 \times 50 \text{ cm}^2$ constructed of clear acrylic sheets. The beam is scanned on one face of the sample and the opposite face is imaged by the CCD. The chamber is placed equidistantly from the CCD and the laser source along the optical axis at a distance of 110 cm. The chamber is filled with a scattering medium which consists of a suspension of 1% Intralipid in water in which absorbing objects may be suspended.

A tomographic data set is acquired by raster scanning the beam over a 29×29 square lattice with a lattice spacing of 0.5 cm. This yields 841 source positions within a $14 \times 14 \text{ cm}^2$ area centered on the optical axis. For each source, a 429×429 pixel region of interest is read out from the CCD. This results in 184,041 detectors arranged in a square lattice with an effective lattice spacing equivalent to 0.065 cm and all detectors located within a $28 \times 28 \text{ cm}^2$ area centered on the optical axis. Thus a data set of 1.5×10^8 source-detector pairs is acquired.

The inverse problem in OT consists of reconstructing $\delta\alpha$ from measurements of ϕ . In this Letter, we consider the inversion of the integral equation (2) in the slab measurement geometry. The approach taken is to construct the singular value decomposition of the integral operator whose kernel is defined by (2) and to use this result to obtain the pseudoinverse solution to (2).

The starting point for this development is to consider the lattice Fourier transform of the sampled data function which is defined by

$$\tilde{\phi}(\mathbf{q}_1, \mathbf{q}_2) = \sum_{\mathbf{r}_1, \mathbf{r}_2} \exp[i(\mathbf{q}_1 \cdot \mathbf{r}_1 + \mathbf{q}_2 \cdot \mathbf{r}_2)] \phi(\mathbf{r}_1, \mathbf{r}_2), \quad (4)$$

where the sum is carried out over the square lattices of sources and detectors with lattice spacings h_1 and h_2 , respectively. The wave vectors \mathbf{q}_1 and \mathbf{q}_2 belong to the

first Brillouin zones of the corresponding lattices, denoted $\text{FBZ}(h_1)$ and $\text{FBZ}(h_2)$. It can then be shown that the pseudoinverse solution to the integral equation (2) is given by the inversion formula

$$\delta\alpha(\mathbf{r}) = \int_{\text{FBZ}(h_1)} d^2q \int_{\text{FBZ}(h_2)} d^2p K(\mathbf{r}; \mathbf{q}, \mathbf{p}) \tilde{\phi}(\mathbf{q} - \mathbf{p}, \mathbf{p}), \quad (5)$$

where the kernel K is defined in Ref. [12]. Several aspects of Eq. (5) are important to note. First, the transverse spatial resolution of reconstructed images is determined by the spatial frequency of sampling of the data function with respect to both source and detector coordinates. As a consequence, a large number of source-detector pairs is required to achieve the highest possible spatial resolution. It can be seen that when the source and detector lattices have equal spacing, the theoretical limit of transverse resolution is given by the lattice spacing. When the source and detector lattice spacings are different, as is the case in the experiment reported here (where $h_1 = 0.5 \text{ cm}$ and $h_2 = 0.065 \text{ cm}$), the resolution of reconstructed images is controlled by the larger lattice spacing (lower spatial frequency). Second, the inverse problem in OT is evidently overdetermined. In addition, it is highly ill-posed. As a result, it can be said that large data sets allow for averaging the data function in such a way that the sensitivity to noise in the inverse problem is partially ameliorated. Finally, numerical implementation of (5) requires replacing the integrals over d^2q and d^2p by sums over a finite set of wavevectors. In practice, we find that integration over d^2q can be carried out with a step size $\Delta q = 0.07 \text{ cm}^{-1}$ and 14,641 integration points while the integration over d^2p requires a step size $\Delta p = 1/2\Delta q$ and 1,296 integration points. Thus a total of 1.9×10^7 Fourier components of the data are used in the reconstruction.

The first step in the reconstruction of tomographic images is to measure the reference intensity I_0 for each source-detector pair. By fitting this data in the spatial frequency domain to (3) with $\alpha = \alpha_0$ we obtain the diffuse wavenumber $k_0 = \sqrt{\alpha_0/D} = 0.58 \text{ cm}^{-1}$ and the extrapolation length $\ell = 0.7 \text{ cm}$. Note that these parameters define the diffusion Green's function G in the slab geometry [10] and that α_0 and D cannot be separately determined from a continuous-wave measurement at a single wavelength. Next, the object to be imaged is placed in the sample chamber and the intensity I for each source-detector pair is measured. In Fig. 2 we show the reconstruction of a pair of black metal balls. The balls have a diameter of 8 mm and were suspended in the midplane of the sample chamber at a constant height with a separation of 3.2 cm. Tomographic images were reconstructed with a $15 \times 15 \text{ cm}^2$ field of view using 230×230 pixels per image with a separation between the slices of 0.26 cm. It can be seen in the central slice, which is equidistant from the source and detector planes, that the balls are well resolved. The shallower and deeper slices show that the balls remain well resolved but with a smaller diameter, as expected. Fig. 3 is a plot of $\delta\alpha/\alpha_0$ along the line passing

through the centers of both balls in the central slice. The distance between the peaks is 3.3 cm in close agreement with the measured separation of the balls. The FWHM of the peaks is 1.1 cm which slightly overestimates the diameter of the balls. The FWHM of the peaks in the depth direction is 1.5 cm (graph not shown). It is important to note that the reconstructed contrast in $\delta\alpha$ is not expected to be quantitative due to the possible breakdown of (2) in the interior of the strongly absorbing balls. Interestingly, however, the shape and volume of the spherical absorbers is recovered well.

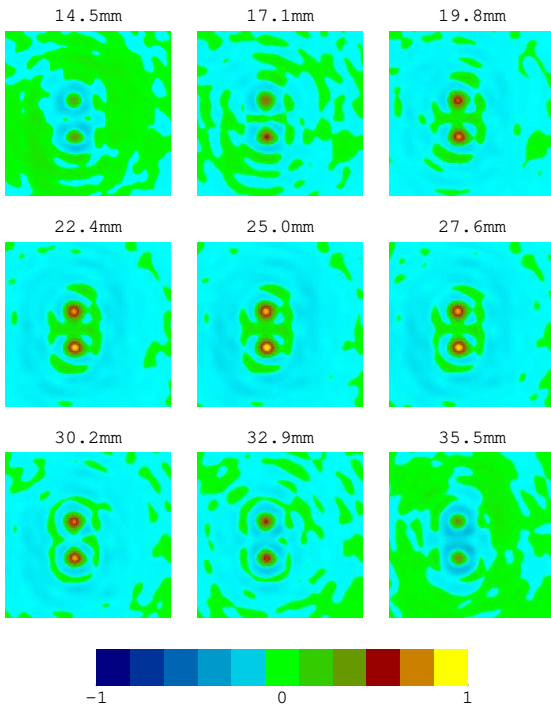


Fig. 2. Reconstructions of $\delta\alpha$ for the two-ball phantom plotted on a linear color scale. The distance of each slice from

the plane of sources is indicated. All images are normalized to the maximum of the central slice.

In conclusion, we have demonstrated the feasibility of analytic methods for image reconstruction in OT with large data sets. We are currently conducting further studies to assess the effects of absorption contrast on image resolution. In addition, the recent availability of CCDs with faster data acquisition will allow the collection of data sets with greater numbers of sources, leading to improvements in spatial resolution. We expect that with further technological advances, resolution consistent with the results of numerical simulations [11] will be achieved.

This research was funded by the NIH under the grants P41RR02305 and R21EB004524. Support from the Whitaker Foundation is also gratefully acknowledged.

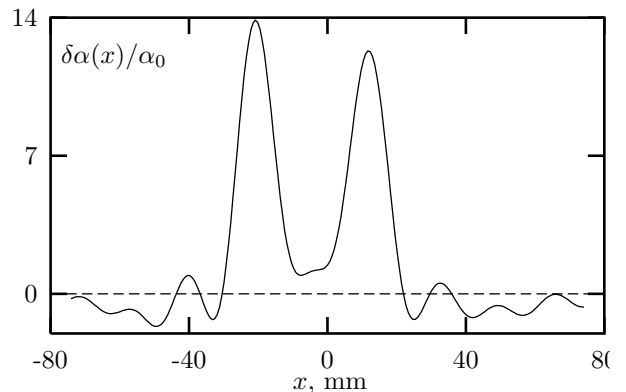


Fig. 3. A one-dimensional profile of the reconstructed absorption along the line passing through the centers of the balls in the central slice.

-
- [1] A. Gibson, J. Hebden and S. Arridge, *Phys. Med. Biol.* **50**, R1 (2005).
 - [2] F. Schmidt, M. Fry, E. Hillman, J. Hebden and D. Delpy, *Rev. Sci. Instruments* **71**, 256 (2000).
 - [3] T. McBride, B. Pogue, S. Jiang, U. Osterberg and K. Paulsen, *Rev. Sci. Instruments* **72**, 1817 (2001).
 - [4] S. Colak, M. van der Mark, G. Hooft, J. Hoogenraad, E. van der Linden, F. Kuijpers, *IEEE J. Selected Topics in Quantum Electronics* **5**, 1143 (1999).
 - [5] R. Schulz, J. Ripoll and V. Ntziachristos, *Opt. Lett.* **28**, 1701 (2003).
 - [6] J. Ripoll and V. Ntziachristos, *Modern Physics Letters B* **18**, 1403 (2004).
 - [7] G. Turner, G. Zacharakis, A. Soubret, J. Ripoll, and V. Ntziachristos, *Opt. Lett.* **30**, 409 (2005).
 - [8] D. Cuccia, F. Bevilacqua, A. Durkin and B. Tromberg, *Opt. Lett.* (in press).
 - [9] J.C. Schotland, *J. Opt. Soc. Am. A* **14**, 275 (1997).
 - [10] V. Markel and J. Schotland, *J. Opt. Soc. Am. A* **19**, 558 (2002).
 - [11] V.A. Markel and J.C. Schotland, *App. Phys. Lett.* **81**, 1180 (2002).
 - [12] V.A. Markel and J.C. Schotland, *Phys. Rev. E* **70**, 056616 (2004).